

Article

Discovery and Biological Evaluation of a Series of Pyrrolo[2,3-*b*]pyrazines as Novel FGFR Inhibitors

Yan Zhang^{1,2}, Hongchun Liu², Zhen Zhang^{3,4}, Ruifeng Wang^{3,4}, Tongchao Liu^{3,4}, Chaoyun Wang¹, Yuchi Ma^{3,*}, Jing Ai^{2,*}, Dongmei Zhao⁴, Jingkang Shen³ and Bing Xiong^{3,*}

¹ School of Pharmaceutical Sciences, Binzhou Medical University, Yantai 264003, China; zhangyanzy2014@126.com (Y.Z.); ytwcy@163.com (C.W.)

² Division of Anti-Tumor Pharmacology, State Key Laboratory of Drug Research, Shanghai Institute of Materia Medica, Chinese Academy of Sciences, 555 Zuchongzhi Road, Shanghai 201203, China; hchliu@simm.ac.cn

³ Department of Medicinal Chemistry, State Key Laboratory of Drug Research, Shanghai Institute of Materia Medica, Chinese Academy of Sciences, 555 Zuchongzhi Road, Shanghai 201203, China; 18204012193@163.com (Z.Z.); rfwang1992@126.com (R.W.); Tongchao_Liu@163.com (T.L.); jkshen@simm.ac.cn (J.S.)

⁴ Key Laboratory of Structure-Based Drug Design & Discovery of Ministry of Education, Shenyang Pharmaceutical University, Shenyang 110016, China; dongmeiz-67@163.com

* Correspondence: ychma@simm.ac.cn (Y.M.); jai@simm.ac.cn (J.A.); bxiong@simm.ac.cn (B.X.); Tel.: +86-21-5080-6600 (ext. 5412) (Y.M.&B.X.); +86-21-5080-6600 (ext. 2413) (J.A.); Fax: +86-21-5080-7088 (Y.M.&B.X.)

Abstract: Abnormality of fibroblast growth factor receptors (FGFRs) mediated signaling pathways were frequently found in various human malignancies, making FGFRs hot targets for cancer treatment. To address the consistent need of new chemotype of FGFR inhibitors, here, we started with a hit structure identified from our internal c-Met inhibitor project, and conducted a chemical optimization. After exploring three parts of the hit compound, we finally discovered a new series of pyrrolo[2,3-*b*] pyrazine FGFR inhibitors, which contain a novel scaffold and unique molecular shape. We believed that our findings can benefit others to further develop selective FGFR inhibitors.

Keywords: FGFR1; inhibitor; kinase inhibitor; pyrazine; hinge binder

1. Introduction

In human genome total 22 fibroblast growth factors (FGFs) were identified and there are four fibroblast growth factor receptors (FGFRs) response and mediate the signaling from fibroblast growth factors[1–4]. Increasing evidences highlight the importance of FGFR signaling pathways in regulation of several basic biologic processes, including tissue development, angiogenesis, and tissue regeneration[5,6]. Not surprising, the abnormal signaling involving FGFRs were frequently found in various human malignancies, making FGFRs hot targets in anticancer drug development[7–9]. Aberrant FGFR signaling could be caused by different mechanisms, including activating mutations in FGFRs, oncogenic fusion of FGFRs and over-expression of FGFRs[10]. Currently, several FGFR-targeted agents, mostly are small molecules binding to the kinase domain, are evaluated in clinical trials for cancer treatment, and most intriguing and advanced evaluated are FGFR-selective inhibitors, such as AZD4547 (1)[11], NVP-BGJ398 (2)[12] and JNJ-42756493 (3)[13]. As investigated by Patani et al.[14], due to the landscape of activated mutations in FGFR kinases, the above-mentioned FGFR inhibitors (1, 2, 3) showed distinct effects towards different mutants, which indicated that developing FGFR inhibitors with novel scaffold are highly demanded as they may provide unique therapeutic benefits towards certain patients.

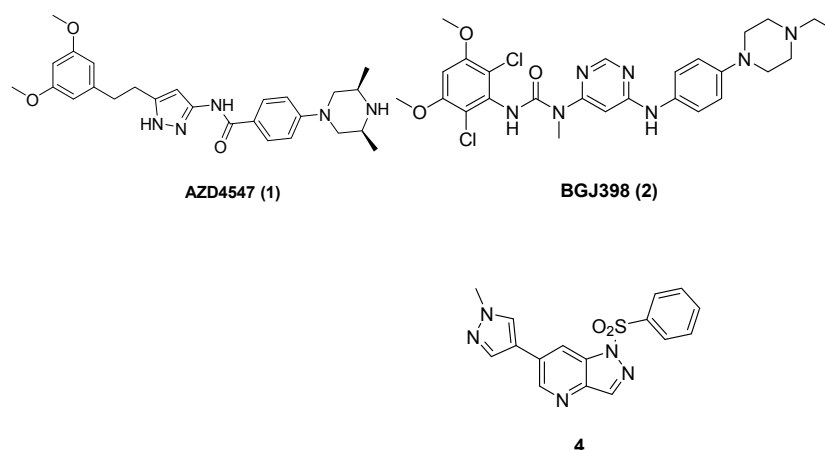


Figure 1. Representative selective FGFR inhibitors.

In the development of tyrosine kinase inhibitors, we previously synthesized a series of 1-sulfonylpyrazolo[4,3-*b*]pyridines as potent and selective c-Met inhibitors[15]. Since c-Met and FGFR are all belong to receptor tyrosine kinase subfamily, we also tested a subset of this series of compounds in an FGFR enzymatic assay and serendipitously found compound **4** showing weak but definite FGFR1 activity, with 87.8% inhibition ratio towards FGFR1 at 10 μ M concentration. Starting from this compound, in current study, we presented our structure optimization and elaborated the structure-activity relationship (SAR) of this novel scaffold, hoping the investigation can stimulate new ideas for developing selective FGFR inhibitors as anticancer drugs.

2. Results and Discussion

As reported in c-Met inhibitor development[15], the 1-sulfonylpyrazolo[4,3-*b*]pyridine acts as the hinge binder, the benzene group of compound **4** forms a π - π interaction with the residue Tyr1230 in the c-Met ATP binding site. Since compound **4** is a novel FGFR inhibitor, both from the view of chemical ring system and from the shape of the structure, we need to probe the binding mode of it. Therefore, We adopted docking study to predict the binding mode of compound **4** in FGFR1 ATP binding site prepared from PDB structure (PDB code: 3TT0)[16]. As shown in Figure 2, the docking result indicated that the pyrazolo[4,3-*b*]pyridine ring still acts as the hinge binder to anchor the molecule in the ATP binding site of FGFR1. Therefore, the benzene group locates at the middle of the ATP binding site and the linking sulfamide group makes it perpendicular to the pyrazolo[4,3-*b*]pyridine. We inspected the predicted complex structure of **4** bound to FGFR1 kinase and did not find any possible residues could form the π - π interaction with benzene group of compound **4**. Then, we designed other three compounds by modifying the connecting group of sulfamide. As shown in Table 1, three compounds showed moderate inhibitions towards FGFR1, but the activities are all inferior to the starting compound **4**. This indicated that the nearly right angle between the benzene group and pyrazolo[4,3-*b*]pyridine ring is important to the binding affinity. Together with the unique shape of compound **4**, we desired to retain this connecting group for late optimization.

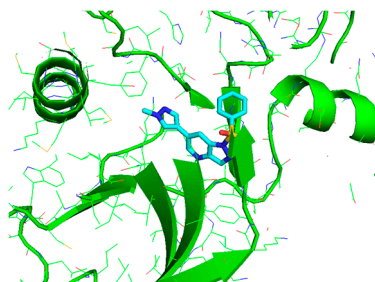
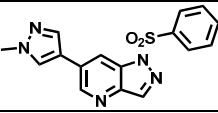
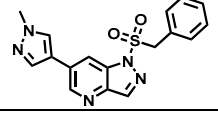
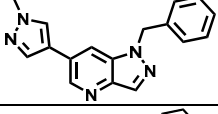
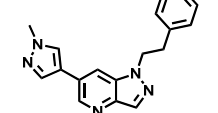


Figure 2. The docking study of compound **4** in FGFR1 binding site. The protein structure was extracted from PDB structure (3TT0), and showing in green color, while compound **4** was depicted in stick model and colored cyan.

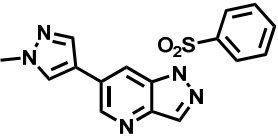
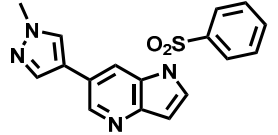
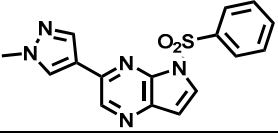
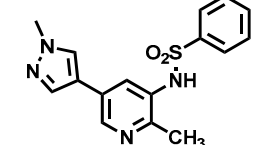
Table 1. Structures and FGFR1 enzymatic activities of compounds 4–7^a.

Compound No.	Structure	FGFR1 Inhibition (%) ^b	
		10 μ M	
4		87.8	
5		46.1	
6		53	
7		55.9	

^aIn our enzymatic assay, the IC_{50} value of AZD4547 on FGFR1 is 1.8 ± 0.1 nM (mean \pm SD). ^bInhibition values are given as the mean (%) from two separate experiments.

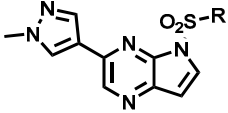
Most of the tyrosine kinase inhibitors comprise a hydrogen bonding acceptor to interact with the hinge part of kinase domain, which is to mimic the binding pattern of adenine group of ATP molecule [17]. Since the hinge binder forms hydrogen bonding and Van der Waals interactions with the binding site residues, it makes a great contribution to anchor the whole inhibitor in the kinase domain. Therefore, we modified it with the aim to improve the binding activity. We retained the important nitrogen atom as hydrogen bond receptor to the backbone of the residue ALA564 and synthesized three compounds listed in Table 2. Changing the scaffold into the 1*H*-pyrrolo[3,2-*b*]pyridine ring (8) slightly decreased the binding activity, while changing into 5*H*-pyrrolo[2,3-*b*]pyrazine (9) dramatically increase the binding activity. Even at the concentration of 1 μ M, it still showed more than 90% inhibition in the FGFR1 enzymatic assay [18,19]. We also changed the bicyclic scaffold into monocycle ring by opening the pyrrole (10), and the activity dropped down about 10-fold, as indicated by the inhibition ratio in Table 2.

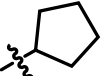
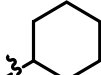
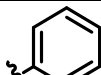
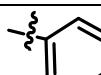
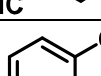
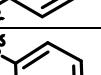
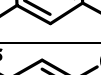
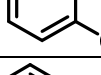
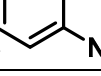
Table 2. Structures and FGFR1 enzymatic activities of compounds 8–10.

Compound No.	Structure	FGFR1 Inhibition (%)	
		10 μ M	1 μ M
4		87.8	47.1
8		80.4	31.6
9		93.3	92.5
10		50.0	15.4

Although we didn't observed any possible residues could make direct interaction with the benzene group of compound **4** by looking the cocrystal structure (pdb code: 3TT0), we are aware that protein kinase domain has a complex conformational landscape, which has been extensively studied by crystal structure analyses and computer simulations[20–22]. Then, by analogy to developing c-Met inhibitors, we optimized the benzene group and synthesized over a dozen compounds listed in Table 3, and indeed found that this part is critical to the binding affinity. Substitution of the benzene group with saturated cyclopentane (**11**) or cyclohexane (**12**) dramatically decreased the binding activity. Generally, the electronic properties of substituents on benzene group are not essential to the binding, if comparing compounds **17** and **19** to compound **9**. These compounds are showing similar sub-micromolar enzymatic activities. By scrutiny of the structure-activity relationship, we found that the steric characteristics may be more important, and the meta-position on the benzene sulfamide is favorable for the binding, which is evident from the comparison of compounds **17** and **18**, or **19** and **20**. The slightly large substitution such as acetyl group (**21**) on meta-position of benzene is also tolerated, while larger propionyl group (**22**) decreased the activity. These reinforce that the steric characteristics of the inhibitors are vital to the binding interactions. From the exploration of this part, we found that the compound containing nitrobenzene group (**17**) stood out as a potent inhibitor with enzymatic activity about 85 nM. Then, this substructure pattern was retained and the methyl pyrazole group was subjected to further optimization.

Table 3. Structures and FGFR1 enzymatic activities of compounds **11–22**.



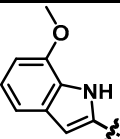
Compound No.	R	FGFR1 Inhibition(%)		
		10 μ M	1 μ M	0.1 μ M
11		34.7	20.8	26.8
12		53.3	24.1	29.4
9		90.5	63.4	46
13		59.7	32.6	40.3
14		45.2	27.2	22
15		55.6	31.2	23.6
16		74.5	34.8	13.6
17		92.1	76.4	61.1
18		15.5	12.8	17.4

19		82.2	57.5	34.7
20		42.4	24.2	31.8
21		79	50.9	44.7
22		38.7	17.3	27.7

To probe the SAR around the methyl pyrazole part, we synthesized analogs **23–25** by substituting methyl group with different acyl groups. When R group is 1-(1*H*-pyrazol-1-yl)ethan-1-one (**23**) or 1-(1*H*-pyrazol-1-yl)propan-1-one (**24**), it showed reduced activity, giving less than 40% inhibition ratio at the concentration of 0.1 μ M. While the compound with 1-(1*H*-pyrazol-1-yl)propan-2-one (**25**) has the similar activity to compound **17**. Modifying the methyl pyrazole to benzene groups (**26**, **27**) follows the similar trend, being that the phenylmethanol substitution (**27**) is more active than the acetophenone substitution (**26**). In general, the modification at the methyl pyrazole part did not improve the binding activity, and only **25** and **27** were found with similar potency to compound **17**, with IC₅₀ values of 45 nM and 113 nM, respectively.

Table 4. Structures and FGFR1 enzymatic activities of compounds **23–28**.

Compound No.	R	FGFR1 Inhibition(%)		
		1 μ M	0.1 μ M	0.01 μ M
17		76.4	61.1	ND
23		58.8	37.8	36.5
24		60.9	30.2	29.3
25		63.4	55.7	32.8
26		57.9	35.7	ND
27		75.5	52.2	ND

28		62.4	34	27.2
----	---	------	----	------

Since this series of compounds are started from the project of developing c-Met inhibitors, we want to assess the selectivity of this series. So three potent compounds were picked to test in c-Met enzymatic assay. As shown in Table 5, three compounds demonstrated nearly no inhibition towards c-Met even at concentration of 1 μ M, indicating compounds of this series may be selective FGFR inhibitors.

Table 5. FGFR1 and c-Met enzymatic activities of compounds 18,25,27.

Compound No.	FGFR1 IC ₅₀ (nM) ^a	c-Met Inhibition(%)		
		1 μ M	0.1 μ M	0.01 μ M
17	85.9 \pm 21.2	30.6	-1.5	-5.4
25	45.9 \pm 14.5	14.1	5.0	5.5
27	113.8 \pm 5.8	30.1	8.4	1.1

^a IC₅₀ values are given as the mean \pm SD (nM) from two separate experiments.

3. Materials and Methods

3.1. Elisa Kinase Assay

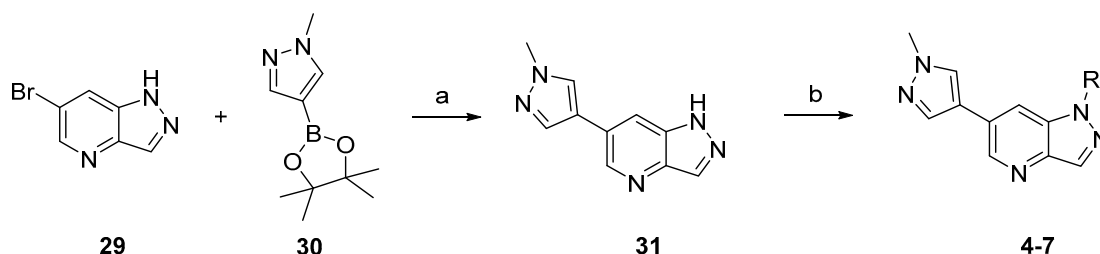
The effects of compounds on the activities of indicated (FGFR1 and c-Met) kinases were determined using enzyme-linked immunosorbent assays (ELISAs) with purified recombinant proteins[19]. Briefly, 20 μ g/mL poly (Glu, Tyr)_{4:1} (Sigma, St. Louis, MO, USA) was pre-coated in 96-well plates as a substrate. A 50- μ L aliquot of 10 μ mol/L ATP solution diluted in kinase reaction buffer (50 mmol/L HEPES [pH 7.4], 50 mmol/L MgCl₂, 0.5 mmol/L MnCl₂, 0.2 mmol/L Na₃VO₄, and 1 mmol/L DTT) was added to each well; 1 μ L of various concentrations of compounds diluted in 1% DMSO (*v/v*) (Sigma) were then added to each reaction well. DMSO (1%, *v/v*) was used as the negative control. The kinase reaction was initiated by the addition of purified tyrosine kinase proteins FGFR1 (Millipore, Darmstadt, Germany) or c-Met (Millipore) diluted in 49 μ L of kinase reaction buffer. After incubation for 60 min at 37°C, the plate was washed three times with phosphate-buffered saline (PBS) containing 0.1% Tween 20 (T-PBS). Anti-phosphotyrosine (PY99) antibody (100 μ L; 1:500, diluted in 5 mg/mL BSA T-PBS) was then added. After a 30-min incubation at 37°C, the plate was washed three times, and 100 μ L horseradish peroxidase-conjugated goat anti-mouse IgG (1:2000, diluted in 5 mg/mL BSA T-PBS) was added. The plate was then incubated at 37°C for 30 min and washed 3 times. A 100- μ L aliquot of a solution containing 0.03% H₂O₂ and 2 mg/mL *o*-phenylenediamine in 0.1 mol/L citrate buffer (pH 5.5) was added. The reaction was terminated by the addition of 50 μ L of 2 mol/L H₂SO₄ as the color changed, and the plate was analyzed using a multi-well spectrophotometer (SpectraMAX 190, from Molecular Devices, Palo Alto, CA, USA) at 490 nm. The inhibition rate (%) was calculated using the following equation: $[1 - (A_{490}/A_{490\text{Control}})] \times 100\%$. The IC₅₀ values were calculated from the inhibition curves in two separate experiments.

3.2. Docking Study

The BGJ398 bound FGFR1 complex structure (PDB code: 3TT0) was downloaded from PDB database, and prepared with protein preparation module in Schrödinger software package. Then the Glide software was used to build the grid file within FGFR1 ATP binding site. The compound 4 was minimized with OPLS2015 force field, and then it was docked into the FGFR1 ATP site with default XP precision parameters implemented in Glide software. Finally, the best predicted binding conformation of compound 4 was illustrated with Pymol program.

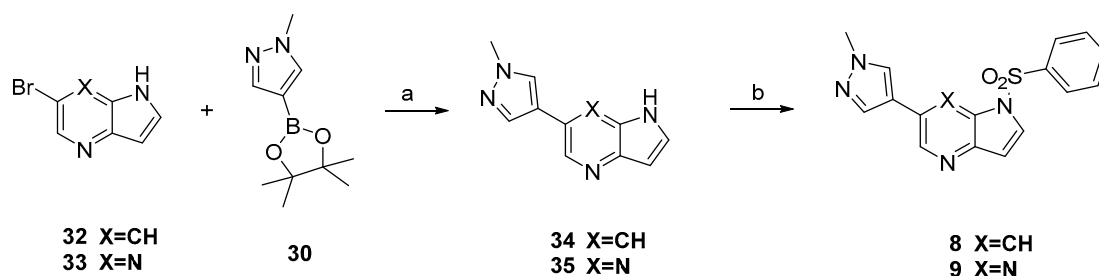
3.3. Chemistry

Compounds 4–7 were synthesized according to the procedures outlined in Scheme 1. Suzuki coupling of commercially available **29** with 1-methylpyrazole-4-boronic acid pinacol ester (**30**) provided **31**. Compounds 4–7 were prepared by deprotonation of compound **31** followed by addition of the corresponding electrophile reagents.



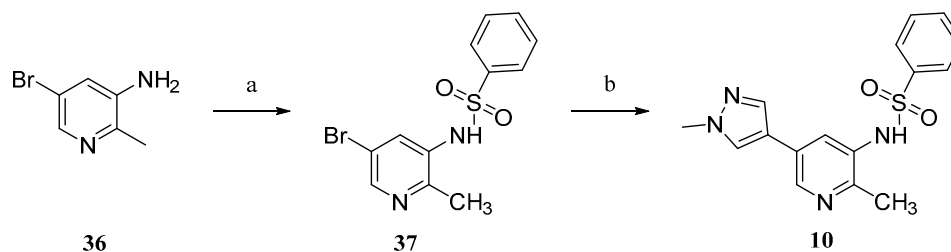
Scheme 1. The synthesis route of compounds 4–7. *Reagents and conditions:* (a) Pd(dppf)Cl₂, K₂CO₃, Dioxane:H₂O (*v/v*=4:1), 80°C, 2 h, 86% yield; (b) NaH, DMF, R-SO₂Cl, r.t., 1–4h, 76%–83% yield.

Compounds **8** and **9** were prepared according to the procedure in Scheme 2. Treatment of compounds **32** and **33** with **30** via Suzuki coupling afforded compounds **34** and **35** which were sulfonated to afford **8** and **9**, respectively.



Scheme 2. The synthesis route of compounds **8** and **9**. *Reagents and conditions:* (a) Pd(dppf)Cl₂, K₂CO₃, Dioxane:H₂O (*v/v*=4:1), 80°C, 3 h, 89% yield(**34**), 82% yield(**35**); (b) NaH, DMF, benzenesulfonyl chloride, r.t., 2 h, 82% yield(**8**), 79% yield(**9**).

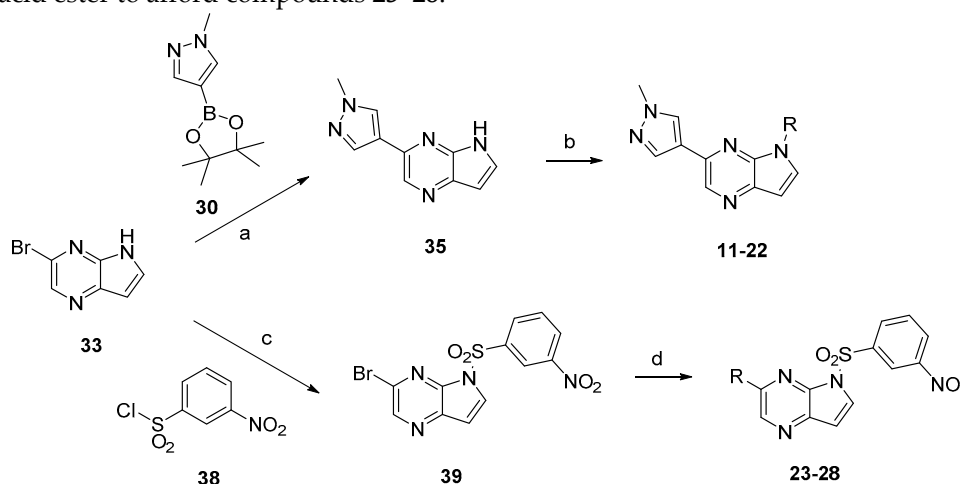
Compound **10** was prepared according to Scheme 3. Commercially available 5-bromo-2-methylpyridin-3-amine (**36**) were sulfonated to afford **37**. Conventional Suzuki coupling of **37** and 1-methylpyrazole-4-boronic acid pinacol ester (**30**) afforded compound **10**.



Scheme 3. The synthesis route of compound **10**. *Reagents and conditions:* (a) benzenesulfonyl chloride, NaH, DMF, r.t., 85% yield; (b) 1-Methylpyrazole-4-boronic acid pinacol ester, Pd(dppf)Cl₂, K₂CO₃, Dioxane:H₂O (*v/v* = 4:1), 80 °C, 3 h, 80% yield.

Compounds **11–28** were prepared according to the procedures outlines in Scheme 4. Compound **33** firstly was treated via Suzuki coupling then sulfonated with corresponding sulfonyl chlorides to afford compounds **11–22**. Correspondingly, compound **33** firstly was sulfonated with

3-nitrobenzenesulfonyl chloride (**38**) then treated via Suzuki coupling with corresponding boric acid or boric acid ester to afford compounds **23–28**.



Scheme 4. The synthesis route of compounds **11–28**. *Reagents and conditions:* (a) Pd(dppf)Cl₂, K₂CO₃, Dioxane:H₂O (*v/v*=4:1), 80°C, 3 h, 82% yield; (b) NaH, DMF, R-SO₂Cl, r.t., 1–4 h, 72%–87% yield; (c) NaH, DMF, r.t., 2 h, 80% yield; (d) Pd(dppf)Cl₂, K₂CO₃, Dioxane:H₂O (*v/v*=4:1), 80°C, 2–4 h, 81%–92% yield.

¹H NMR (400 MHz) and ¹³C-NMR (125 MHz or 151 MHz) spectra were recorded by using a Varian Mercury-400, a Mercury-500 and a Mercury-600 High Performance Digital FT-NMR spectrometer with tetramethylsilane (TMS) as an internal standard. Abbreviations for peak patterns in NMR spectra: br = broad, s = singlet, d = doublet, and m = multiplet. Low-resolution mass spectra were obtained with a Finnigan LCQ Deca XP mass spectrometer using a CAPCELL PAK C18 (50 mm × 2.0 mm, 5 ZM) or an Agilent ZORBAX Eclipse XDB C18 (50 mm × 2.1 mm, 5 ZM) in positive or negative electrospray mode. Purity of all compounds was determined by analytical Gilson high-performance liquid chromatography (HPLC) using an YMC ODS3 column (50 mm × 4.6 mm, 5 ZM). Conditions were as follows: CH₃CN/H₂O eluent at 2.5 mL min⁻¹ flow [containing 0.1% trifluoroacetic acid (TFA)] at 35 °C, 8 min, gradient 5% CH₃CN to 95% CH₃CN, monitored by UV absorption at 214 nm and 254 nm. TLC analysis was carried out with glass precoated silica gel GF254 plates. TLC spots were visualized under UV light. Flash column chromatography was performed with a Teledyne ISCO CombiFlash Rf system. All solvents and reagents were used directly as obtained commercially unless otherwise noted. Anhydrous dimethylformamide was purchased from Acros and was used without further drying. All air and moisture sensitive reactions were carried out under an atmosphere of dry Argon with heat-dried glassware and standard syringe techniques.

6-(1-methyl-1H-pyrazol-4-yl)-1H-pyrazolo[4,3-b]pyridine (31). A solution of 6-bromo-1H-pyrazolo[4,3-b]pyridine (**29**) (330 mg, 1.52 mmol), 1-methyl-4-(4,4,5,5-tetramethyl-1,3,2-dioxaborolan-2-yl)-1H-pyrazole (**30**) (378 mg, 1.82 mmol), PdCl₂(dppf)-CH₂Cl₂ (61.9 mg, 80 μmol) and K₂CO₃ (628 mg, 4.54 mmol) in 1,4-dioxane:water (15 mL, 2:1, *v*) in a microwave tube was flushed with N₂ for 5 mins then sealed. The tube was heated at 80 °C for 2 h. Then the reaction mixture was evaporated to dryness. The residue was purified by flash chromatography to give **31** (260 mg, 86% yield); LC-MS *m/z* (ESI) found (M + H)⁺ 200.0 (M + H)⁺; ¹H NMR (400 MHz, DMSO-*d*₆) δ 13.29 (s, 1H), 8.80 (s, 1H), 8.36 (s, 1H), 8.24 (s, 1H), 8.07 (s, 2H), 3.90 (s, 3 H).

6-(1-methyl-1H-pyrazol-4-yl)-1-(phenylsulfonyl)-1H-pyrazolo[4,3-b]pyridine (4). Sodium hydride (29 mg, 1.2 mmol) was suspended in 3 mL of anhydrous DMF. 6-(1-methyl-1H-pyrazol-4-yl)-1H-pyrazolo[4,3-b]pyridine (**31**) (160 mg, 0.8 mmol) was dissolved in 5 mL of anhydrous DMF was slowly added dropwise, and the mixture was stirred for 30 min. benzenesulfonyl chloride (214 mg, 0.94 mmol) dissolved in 5 mL of anhydrous DMF was slowly added in drops, and the mixture was stirred for 4 h at room temperature. The reaction solution was poured to 0.1 N hydrochloric acid, which was then brought to basic using aqueous sodium bicarbonate solution, and extracted with ethyl acetate. The organic layer was collected, and distilled

under reduced pressure. The remaining substance was purified by flash column chromatography to give **4** (224 mg, 82% yield); LC-MS m/z (ESI) found (M + H)⁺ 340.0 (M + H)⁺; ¹H NMR (400 MHz, Chloroform-*d*) δ 8.84 (d, J = 1.7 Hz, 1 H), 8.49 (s, 1 H), 8.38 (s, 1 H), 8.02 (d, J = 7.4 Hz, 2 H), 7.94 (s, 1H), 7.86 (s, 1H), 7.62 (t, J = 7.4 Hz, 1 H), 7.51 (t, J = 7.8 Hz, 2 H), 4.03 (s, 3 H). Retention time 2.95 min., >98% purity.

Compounds **5-7** were prepared with a similar procedure as that used for **4**.

1-(benzylsulfonyl)-6-(1-methyl-1H-pyrazol-4-yl)-1H-pyrazolo[4,3-b]pyridine (**5**). LC-MS m/z (ESI) found (M + H)⁺ 354.1 (M + H)⁺; ¹H NMR (400 MHz, Chloroform-*d*) δ 8.72 (d, J = 1.9 Hz, 1H), 8.50 (d, J = 0.9 Hz, 1H), 7.74 (d, J = 0.7 Hz, 1H), 7.69 (dd, J = 1.9, 0.8 Hz, 1H), 7.67 (s, 1H), 7.11 – 7.03 (m, 3H), 6.97 (dd, J = 7.9, 1.6 Hz, 2H), 4.70 (s, 2H), 4.00 (s, 3H). Retention time 2.97 min., >98% purity.

1-benzyl-6-(1-methyl-1H-pyrazol-4-yl)-1H-pyrazolo[4,3-b]pyridine (**6**). LC-MS m/z (ESI) found (M + H)⁺ 290.1 (M + H)⁺; ¹H NMR (400 MHz, Chloroform-*d*) δ 8.73 (d, J = 1.8 Hz, 1H), 8.28 (d, J = 0.9 Hz, 1H), 7.81 (s, 1H), 7.72 (s, 1H), 7.64 – 7.59 (m, 1H), 7.38–7.30 (m, 3H), 7.25–7.21 (m, 2H), 5.64 (s, 2H), 4.00 (s, 3H). Retention time 3.05 min., 98.25% purity.

6-(1-methyl-1H-pyrazol-4-yl)-1-phenethyl-1H-pyrazolo[4,3-b]pyridine (**7**). LC-MS m/z (ESI) found (M + H)⁺ 304.1 (M + H)⁺; ¹H NMR (400 MHz, Chloroform-*d*) δ 8.74 (d, J = 1.9 Hz, 1H), 8.06 (d, J = 1.0 Hz, 1H), 7.96 (s, 1H), 7.88 (s, 1H), 7.75 (s, 1H), 7.32–7.24 (m, 3H), 7.14–7.10 (m, 2H), 4.68 (t, J = 7.3 Hz, 2H), 4.01 (s, 3H), 3.35 (t, J = 7.3 Hz, 2H). Retention time 3.08 min., >98% purity.

6-(1-methyl-1H-pyrazol-4-yl)-1H-pyrrolo[3,2-b]pyridine (**34**). A solution of 6-bromo-1H-pyrrolo[3,2-b]pyridine (**32**) (100mg, 0.51 mmol), 1-methyl-4-(4,4,5,5-tetramethyl-1,3,2-dioxaborolan-2-yl)-1H-pyrazole (**30**) (116 mg, 0.56 mmol), PdCl₂(dppf)-CH₂Cl₂ (37 mg, 50 μmol) and K₂CO₃ (140 mg, 1.01 mmol) in 1,4-dioxane:water (6 mL, 2:1, v) in a microwave tube was flushed with N₂ for 5 mins then sealed. The tube was heated at 80 °C for 3 h. Then the reaction mixture was evaporated to dryness. The residue was purified by flash chromatography to give **34** (90 mg, 89% yield); LC-MS m/z (ESI) found (M + H)⁺ 199.1 (M + H)⁺; ¹H NMR (400 MHz, DMSO-*d*₆) δ 11.31 (s, 1H), 8.59 (s, 1H), 8.21 (s, 1H), 7.93 (s, 1H), 7.87 (s, 1H), 7.60 (t, J = 2.8 Hz, 1H), 6.53 (s, 1H), 3.88 (s, 3H).

6-(1-methyl-1H-pyrazol-4-yl)-1-(phenylsulfonyl)-1H-pyrrolo[3,2-b]pyridine (**8**). Sodium hydride (7 mg, 0.28 mmol) was suspended in 3 mL of anhydrous DMF. 6-(1-methyl-1H-pyrazol-4-yl)-1H-pyrrolo[3,2-b]pyridine (**34**) (50 mg, 0.25 mmol) was dissolved in 3 mL of anhydrous DMF was slowly added dropwise, and the mixture was stirred for 30 min. benzenesulfonyl chloride (38 μL, 0.28 mmol) dissolved in 3 mL of anhydrous DMF was slowly added in drops, and the mixture was stirred for 2 h at room temperature. The reaction solution was poured to 0.1 N hydrochloric acid, which was then brought to basic using aqueous sodium bicarbonate solution, and extracted with ethyl acetate. The organic layer was collected, and distilled under reduced pressure. The remaining substance was purified by flash column chromatography to give **8** (70 mg, 82% yield); LC-MS m/z (ESI) found (M + H)⁺ 339.1 (M + H)⁺; ¹H NMR (400 MHz, Chloroform-*d*) δ 8.70 (d, J = 1.7 Hz, 1H), 8.32 (d, J = 1.2 Hz, 1H), 7.91 (s, 1H), 7.89 (t, J = 1.7 Hz, 1H), 7.87–7.85 (m, 1H), 7.77 (d, J = 3.8 Hz, 2H), 7.63–7.56 (m, 1H), 7.49 (t, J = 7.7 Hz, 2H), 6.88 (dd, J = 3.8, 0.7 Hz, 1H), 4.02 (s, 3H). Retention time 2.92 min., >98% purity.

Compounds **9** were prepared with a similar procedure as that used for **8**.

3-(1-methyl-1H-pyrazol-4-yl)-5-(phenylsulfonyl)-5H-pyrrolo[2,3-b]pyrazine (**9**). LC-MS m/z (ESI) found (M + H)⁺ 340.0 (M + H)⁺; ¹H NMR (400 MHz, Chloroform-*d*) δ 8.71 (s, 1H), 8.28–8.19 (m, 2H), 8.09 (s, 1H), 8.03 (s, 1H), 7.94 (d, J = 4.1 Hz, 1H), 7.62 (d, J = 7.4 Hz, 1H), 7.54 (t, J = 7.7 Hz, 2H), 6.80 (d, J = 4.1 Hz, 1H), 4.04 (s, 3H). ¹³C NMR (126 MHz, Chloroform-*d*) δ 142.22, 140.54, 139.05, 138.04, 137.96, 137.77, 134.47, 129.14 (C×2), 129.10, 128.96, 128.24 (C×2), 120.98, 106.58, 39.37. Retention time 2.99 min., >99% purity.

N-(5-bromo-2-methylpyridin-3-yl)benzenesulfonamide (**37**). To a stirred solution of the 5-bromo-2-methylpyridin-3-amine (**36**) (200 mg, 1.07 mmol) in anhydrous dichloromethane (15 mL) was added benzenesulfonyl chloride (152 μL, 1.12 mmol). After 1h, The mixture was then partially concentrated in vacuo, diluted with EtOAc (40 mL) and saturated NaHCO₃ solution (20 mL) and partitioned. The aqueous layer was extracted with EtOAc (2 x 20 mL). The combined organic layers were dried (Na₂SO₄), filtered and concentrated to afford **37** (300mg, 85% yield); LC-MS m/z (ESI)

found (M + H)⁺ 328.1 (M + H)⁺; ¹H NMR (400 MHz, Chloroform-*d*) δ 8.37 (d, J = 2.1 Hz, 1H), 7.92 (d, J = 2.1 Hz, 1H), 7.82–7.76 (m, 2H), 7.67–7.61 (m, 1H), 7.56–7.49 (m, 2H), 2.17 (s, 3H).

N-(2-methyl-5-(1-methyl-1H-pyrazol-4-yl)pyridin-3-yl)benzenesulfonamide (**10**). A solution of *N*-(5-bromo-2-methylpyridin-3-yl)benzenesulfonamide (**37**) (100mg, 0.31 mmol), 1-methyl-4-(4,4,5,5-tetramethyl-1,3,2-dioxaborolan-2-yl)-1H-pyrazole (**30**) (70 mg, 0.34 mmol), PdCl₂(dppf)-CH₂Cl₂ (20 mg, 24 μmol) and K₂CO₃ (84 mg, 0.61 mmol) in 1,4-dioxane:water (15 mL, 2:1, v) in a microwave tube was flushed with N₂ for 5 mins then sealed. The tube was heated at 80 °C for 3 h. Then the reaction mixture was evaporated to dryness. The residue was purified by flash chromatography to give **10** (80 mg, 80% yield); LC-MS m/z (ESI) found (M + H)⁺ 329.1 (M + H)⁺; ¹H NMR (400 MHz, DMSO-*d*₆) δ 8.45 (d, J = 2.0 Hz, 1H), 7.78–7.75 (m, 2H), 7.73 (d, J = 1.4 Hz, 1H), 7.71 (s, 1H), 7.67 (s, 1H), 7.59 (t, J = 7.5 Hz, 1H), 7.47 (t, J = 7.8 Hz, 2H), 5.30 (s, 1H), 3.97 (s, 3H), 2.16 (s, 3H). Retention time 2.54 min., >98% purity.

Compounds **11-28** were prepared with a similar procedure as that used for **8**.

3-(1-methyl-1H-pyrazol-4-yl)-5H-pyrrolo[2,3-*b*]pyrazine (**35**). LC-MS m/z (ESI) found (M + H)⁺ 199.1 (M + H)⁺; ¹H NMR (400 MHz, DMSO-*d*₆) δ 9.30 (s, 1H), 8.72 (s, 1H), 8.11 (s, 1H), 7.97 (s, 1H), 7.28 (s, 1H), 6.74 (dd, J = 3.7, 1.9 Hz, 1H), 4.02 (s, 3H).

5-(cyclopentylsulfonyl)-3-(1-methyl-1H-pyrazol-4-yl)-5H-pyrrolo[2,3-*b*]pyrazine(**11**). LC-MS m/z (ESI) found (M + H)⁺ 311.2 (M + H)⁺; ¹H NMR (400 MHz, Chloroform-*d*) δ 8.80 (s, 1H), 8.09 (d, J = 0.8 Hz, 1H), 8.07 (s, 1H), 7.83 (d, J = 4.1 Hz, 1H), 6.83 (d, J = 4.1 Hz, 1H), 4.03 (s, 3H), 3.16–3.01 (m, 1H), 2.20 (m, 2H), 2.01 (m, 2H), 1.96–1.62 (m, 4H). Retention time 2.57 min., >99% purity.

5-(cyclohexylsulfonyl)-3-(1-methyl-1H-pyrazol-4-yl)-5H-pyrrolo[2,3-*b*]pyrazine (**12**). LC-MS m/z (ESI) found (M + H)⁺ 345.1 (M + H)⁺; ¹H NMR (400 MHz, Chloroform-*d*) δ 8.81 (s, 1H), 8.07 (d, J = 0.8 Hz, 1H), 8.05 (s, 1H), 7.84 (d, J = 4.1 Hz, 1H), 6.85 (d, J = 4.1 Hz, 1H), 4.01 (s, 3H), 3.82 (m, 1H), 2.01–1.85 (m, 4H), 1.69 (dd, J = 10.9, 4.8 Hz, 2H), 1.32–1.17 (m, 4H). Retention time 2.59 min., 98.54% purity.

2-((3-(1-methyl-1H-pyrazol-4-yl)-5H-pyrrolo[2,3-*b*]pyrazin-5-yl)sulfonyl)benzotrile(**13**). LC-MS m/z (ESI) found (M + H)⁺ 364.0 (M + H)⁺; ¹H NMR (400 MHz, Chloroform-*d*) δ 8.71 (s, 1H), 8.66–8.62 (m, 1H), 8.16 (d, J = 4.2 Hz, 1H), 8.01–7.96 (m, 2H), 7.89–7.83 (m, 2H), 7.77 (dd, J = 7.6, 1.3 Hz, 1H), 6.89 (d, J = 4.2 Hz, 1H), 4.02 (s, 3H). ¹³C NMR (126 MHz, Chloroform-*d*) δ 142.29, 140.40, 139.90, 139.20, 138.37, 137.78, 135.52, 134.39, 132.82, 131.76, 130.15, 129.00, 120.65, 115.00, 111.37, 106.99, 39.36. Retention time 3.04 min., >99% purity.

5-((4-chlorophenyl)sulfonyl)-3-(1-methyl-1H-pyrazol-4-yl)-5H-pyrrolo[2,3-*b*]pyrazine(**14**). HPLC 96.66%; LC-MS m/z (ESI) found (M + H)⁺ 373.0 (M + H)⁺; ¹H NMR (400 MHz, Chloroform-*d*) δ 8.73 (s, 1H), 8.19 (d, J = 8.5 Hz, 2H), 8.09 (s, 1H), 8.03 (s, 1H), 7.91 (d, J = 4.1 Hz, 1H), 7.51 (d, J = 8.5 Hz, 2H), 6.82 (d, J = 4.1 Hz, 1H), 4.05 (s, 3H). Retention time 2.98 min., 96.66% purity.

5-((2,4-difluorophenyl)sulfonyl)-3-(1-methyl-1H-pyrazol-4-yl)-5H-pyrrolo[2,3-*b*]pyrazine(**15**). LC-MS m/z (ESI) found (M + H)⁺ 375.1 (M + H)⁺; ¹H NMR (400 MHz, Chloroform-*d*) δ 8.71 (s, 1H), 8.44 (td, J = 8.5, 8.5, 6.0 Hz, 1H), 8.01 (dd, J = 4.1, 1.3 Hz, 1H), 7.99 (d, J = 0.7 Hz, 1H), 7.91 (s, 1H), 7.16–7.10 (m, 1H), 6.90 (ddd, J = 10.4, 8.3, 2.4 Hz, 1H), 6.85 (d, J = 4.1 Hz, 1H), 4.02 (s, 3H). Retention time 2.97 min., 94.53% purity.

5-((3,4-dichlorophenyl)sulfonyl)-3-(1-methyl-1H-pyrazol-4-yl)-5H-pyrrolo[2,3-*b*]pyrazine(**16**). LC-MS m/z (ESI) found (M + H)⁺ 407.0 (M + H)⁺; ¹H NMR (400 MHz, Chloroform-*d*) δ 8.75 (s, 1H), 8.50 (d, J = 2.2 Hz, 1H), 8.10 (d, J = 0.7 Hz, 1H), 8.06 (s, 1H), 8.03 (dd, J = 8.5, 2.2 Hz, 1H), 7.90 (d, J = 4.1 Hz, 1H), 7.62 (d, J = 8.5 Hz, 1H), 6.84 (d, J = 4.2 Hz, 1H), 4.06 (s, 3H). ¹³C NMR (126 MHz, Chloroform-*d*) δ 142.44, 140.33, 139.75, 139.07, 138.37, 137.69, 137.34, 133.79, 131.27, 130.76, 129.06, 128.62, 127.09, 120.71, 107.13, 39.38. Retention time 3.02 min., >99% purity.

3-(1-methyl-1H-pyrazol-4-yl)-5-((3-nitrophenyl)sulfonyl)-5H-pyrrolo[2,3-*b*]pyrazine(**17**). LC-MS m/z (ESI) found (M + H)⁺ 384.2 (M + H)⁺; ¹H NMR (400 MHz, Chloroform-*d*) δ 9.40 (t, J = 2.1, 2.1 Hz, 1H), 8.77 (s, 1H), 8.49 (dd, J = 10.8, 8.0 Hz, 2H), 8.24 (s, 1H), 8.06 (s, 1H), 7.92 (d, J = 4.2 Hz, 1H), 7.78 (t, J = 8.1, 8.1 Hz, 1H), 6.86 (dd, J = 4.2, 0.7 Hz, 1H), 4.08 (s, 3H). ¹³C NMR (126 MHz, Chloroform-*d*) δ 148.09, 142.68, 140.32, 139.87, 139.00, 138.45, 137.37, 133.39, 130.67, 129.68, 128.93, 128.39, 124.61, 120.43, 107.41, 39.37. Retention time 3.01 min., >99% purity.

3-(1-methyl-1H-pyrazol-4-yl)-5-((4-nitrophenyl)sulfonyl)-5H-pyrrolo[2,3-*b*]pyrazine(**18**). LC-MS m/z (ESI) found (M + H)⁺ 384.0 (M + H)⁺; ¹H NMR (400 MHz, Chloroform-*d*) δ 8.75 (s, 1H), 8.48–8.44 (m, 2H),

8.37 (d, $J = 8.8$ Hz, 2H), 8.10 (s, 1H), 8.03 (s, 1H), 7.91 (d, $J = 4.1$ Hz, 1H), 6.87 (d, $J = 4.1$ Hz, 1H), 4.06 (s, 3H). Retention time 3.02 min., 98.86% purity.

3-((3-(1-methyl-1H-pyrazol-4-yl)-5H-pyrrolo[2,3-b]pyrazin-5-yl)sulfonyl)aniline(**19**). LC-MS m/z (ESI) found (M + H)⁺ 354.1 (M + H)⁺; ¹H NMR (600 MHz, Chloroform-*d*) δ 9.05 (d, $J = 1.9$ Hz, 1H), 8.67 (s, 1H), 8.17–8.14 (m, 2H), 8.06 (dd, $J = 8.5, 0.8$ Hz, 1H), 8.04 (d, $J = 0.8$ Hz, 1H), 7.98 (d, $J = 4.1$ Hz, 1H), 7.42 (d, $J = 8.4$ Hz, 1H), 6.80 (d, $J = 4.1$ Hz, 1H), 4.05 (s, 3H). Retention time 2.79 min., 94.56% purity.

4-((3-(1-methyl-1H-pyrazol-4-yl)-5H-pyrrolo[2,3-b]pyrazin-5-yl)sulfonyl)aniline(**20**). LC-MS m/z (ESI) found (M + H)⁺ 355.07 (M + H)⁺; ¹H NMR (400 MHz, Chloroform-*d*) δ 8.69 (s, 1H), 8.09 (d, $J = 0.8$ Hz, 1H), 8.03 (s, 1H), 8.01 (d, $J = 2.0$ Hz, 1H), 7.99 (d, $J = 2.0$ Hz, 1H), 7.93 (d, $J = 4.1$ Hz, 1H), 6.76 (d, $J = 4.1$ Hz, 1H), 6.66 (d, $J = 2.0$ Hz, 1H), 6.64 (d, $J = 2.0$ Hz, 1H), 4.04 (s, 3H). Retention time 2.75 min., 98.68% purity.

N-(3-((3-(1-methyl-1H-pyrazol-4-yl)-5H-pyrrolo[2,3-b]pyrazin-5-yl)sulfonyl)phenyl)acetamide(**21**). HPLC 94.55%; LC-MS m/z (ESI) found (M + H)⁺ 396.1 (M + H)⁺; ¹H NMR (400 MHz, Chloroform-*d*) δ 8.72 (s, 1H), 8.61 (s, 1H), 8.20 (s, 1H), 8.06 (s, 1H), 7.91 (t, $J = 6.0, 6.3$ Hz, 2H), 7.66 (d, $J = 8.2$ Hz, 1H), 7.47 (d, $J = 8.1$ Hz, 1H), 7.44 (d, $J = 12.3$ Hz, 1H), 6.80 (d, $J = 4.1$ Hz, 1H), 4.01 (s, 3H), 2.04 (s, 3H). Retention time 3.12 min., 94.55% purity.

N-(3-((3-(1-methyl-1H-pyrazol-4-yl)-5H-pyrrolo[2,3-b]pyrazin-5-yl)sulfonyl)phenyl)propionamide(**22**). LC-MS m/z (ESI) found (M + H)⁺ 410.1 (M + H)⁺; ¹H NMR (400 MHz, Chloroform-*d*) δ 8.71 (s, 1H), 8.61 (s, 1H), 8.22 (s, 1H), 8.07 (s, 1H), 7.92 (t, $J = 6.1, 6.1$ Hz, 2H), 7.67 (d, $J = 8.3$ Hz, 1H), 7.47 (d, $J = 8.1$ Hz, 1H), 7.42 (d, $J = 12.5$ Hz, 1H), 6.81 (d, $J = 4.1$ Hz, 1H), 4.04 (s, 3H), 2.41 (q, $J = 7.6, 7.6, 7.6$ Hz, 2H), 1.24 (t, $J = 7.4, 7.4$ Hz, 3H). Retention time 3.13 min., 97.72% purity.

1-(4-(5-((3-nitrophenyl)sulfonyl)-5H-pyrrolo[2,3-b]pyrazin-3-yl)-1H-pyrazol-1-yl)ethan-1-one(**23**). LC-MS m/z (ESI) found (M + H)⁺ 412.0 (M + H)⁺; ¹H NMR (400 MHz, Chloroform-*d*) δ 9.28 (s, 1H), 8.91 (s, 1H), 8.86 (s, 1H), 8.58 (d, $J = 8.0$ Hz, 1H), 8.51 (d, $J = 8.2$ Hz, 1H), 8.40 (s, 1H), 8.02 (d, $J = 4.2$ Hz, 1H), 7.81 (t, $J = 8.2, 8.2$ Hz, 1H), 6.91 (d, $J = 4.2$ Hz, 1H), 2.83 (s, 3H). ¹³C NMR (126 MHz, Chloroform-*d*) δ 169.38, 148.24, 142.03, 140.64, 140.34, 140.19, 139.73, 139.00, 133.57, 130.68, 129.81, 129.04, 126.08, 124.04, 123.66, 107.39, 21.67. Retention time 2.64 min., 90.95% purity.

1-(4-(5-((3-nitrophenyl)sulfonyl)-5H-pyrrolo[2,3-b]pyrazin-3-yl)-1H-pyrazol-1-yl)propan-1-one(**24**). LC-MS m/z (ESI) found (M + H)⁺ 426.3 (M + H)⁺; ¹H NMR (400 MHz, Chloroform-*d*) δ 9.27 (t, $J = 2.0, 2.0$ Hz, 1H), 8.91 (d, $J = 0.8$ Hz, 1H), 8.86 (s, 1H), 8.61–8.56 (m, 1H), 8.53–8.48 (m, 2H), 8.38 (d, $J = 0.8$ Hz, 1H), 8.32 (s, 1H), 8.02 (d, $J = 4.2$ Hz, 1H), 6.91 (d, $J = 4.2$ Hz, 1H), 3.27 (q, $J = 7.4, 7.4, 7.4$ Hz, 2H), 1.38 (t, $J = 7.4, 7.4$ Hz, 3H). ¹³C NMR (126 MHz, Chloroform-*d*) δ 172.88, 148.25, 141.86, 140.77, 140.28, 139.75, 139.00, 138.69, 133.60, 130.66, 129.74, 129.04, 126.18, 124.36, 124.02, 123.35, 107.39, 29.70. Retention time 2.65 min., 95.32% purity.

1-(4-(5-((3-nitrophenyl)sulfonyl)-5H-pyrrolo[2,3-b]pyrazin-3-yl)-1H-pyrazol-1-yl)propan-2-one(**25**). LC-MS m/z (ESI) found (M + H)⁺ 426.2 (M + H)⁺; ¹H NMR (400 MHz, Chloroform-*d*) δ 9.40 (t, $J = 2.0, 2.0$ Hz, 1H), 8.79 (s, 1H), 8.48 (dddd, $J = 15.5, 8.0, 2.0, 1.0$ Hz, 2H), 8.30 (d, $J = 0.8$ Hz, 1H), 8.14 (d, $J = 0.7$ Hz, 1H), 7.95 (d, $J = 4.1$ Hz, 1H), 7.79 (t, $J = 8.0, 8.0$ Hz, 1H), 6.87 (d, $J = 4.1$ Hz, 1H), 5.11 (s, 2H), 2.29 (s, 3H). ¹³C NMR (151 MHz, Chloroform-*d*) δ 201.10, 147.99, 142.15, 140.19, 139.74, 139.23, 138.40, 138.03, 133.42, 130.72, 130.44, 128.98, 128.59, 124.75, 121.22, 107.31, 61.19, 27.02. Retention time 2.66 min., 94.67% purity.

1-(4-(5-((3-nitrophenyl)sulfonyl)-5H-pyrrolo[2,3-b]pyrazin-3-yl)phenyl)ethan-1-one(**26**). LC-MS m/z (ESI) found (M + H)⁺ 422.3 (M + H)⁺; ¹H NMR (400 MHz, Chloroform-*d*) δ 9.32 (t, $J = 2.0, 2.0$ Hz, 1H), 9.12 (s, 1H), 8.60–8.55 (m, 1H), 8.53–8.48 (m, 1H), 8.25 (d, $J = 8.4$ Hz, 2H), 8.18 (d, $J = 8.4$ Hz, 2H), 8.09 (d, $J = 4.2$ Hz, 1H), 7.79 (t, $J = 8.1, 8.1$ Hz, 1H), 6.96 (d, $J = 4.1$ Hz, 1H), 3.73 (d, $J = 0.8$ Hz, 3H). Retention time 2.65 min., 91.84% purity.

4-(5-((3-nitrophenyl)sulfonyl)-5H-pyrrolo[2,3-b]pyrazin-3-yl)phenyl)methanol(**27**). LC-MS m/z (ESI) found (M + H)⁺ 410.0 (M + H)⁺; ¹H NMR (400 MHz, Chloroform-*d*) δ 9.30 (t, $J = 2.0, 2.0$ Hz, 1H), 9.02 (s, 1H), 8.57 (dt, $J = 7.9, 1.5, 1.5$ Hz, 1H), 8.48 (ddd, $J = 8.2, 2.3, 1.1$ Hz, 1H), 8.13 (d, $J = 1.4$ Hz, 1H), 8.11 (s, 1H), 8.02 (d, $J = 4.2$ Hz, 1H), 7.77 (t, $J = 8.1, 8.1$ Hz, 1H), 7.57 (d, $J = 8.1$ Hz, 2H), 6.91 (d, $J = 4.1$ Hz, 1H), 4.83 (s, 2H). ¹³C NMR (126 MHz, Chloroform-*d*) δ 148.17, 147.07, 142.88, 140.39, 140.11, 139.84, 139.22, 135.31, 133.66, 130.68, 129.64, 128.97, 127.64(C \times 2), 127.20(C \times 2), 124.29, 107.25, 64.85. Retention time 2.71 min., 94.62% purity.

3-(7-methoxy-1H-indol-2-yl)-5-((3-nitrophenyl)sulfonyl)-5H-pyrrolo[2,3-b]pyrazine(28). LC-MS m/z (ESI) found (M + H)⁺ 449.1 (M + H)⁺; ¹H NMR (400 MHz, Chloroform-d) δ 9.43 (s, 1H), 9.19 (s, 1H), 9.07 (s, 1H), 8.58 (s, 1H), 8.50 (s, 1H), 7.99 (s, 1H), 7.81 (s, 1H), 7.23–7.03 (m, 2H), 6.97–6.87 (m, 1H), 6.78 (d, J = 8.4 Hz, 1H), 4.12 (s, 3H). Retention time 2.94 min., 96.21% purity.

4. Conclusions

Starting with the scaffold of 1-sulfonylpyrazolo[4,3-b]pyridine discovered in c-Met inhibitor development, we conducted a hit optimization towards the inhibitory activity of FGFR1. We explored the SAR of this new chemotype on three parts, namely the scaffold, π - π stacking part and methyl pyrazolepart. We found that the scaffold is essential to the binding activity, and substituting the pyrazolo[4,3-b] pyridine withpyrrolo[2,3-b]pyrazine increases about 10 fold of the inhibitory activity on FGFR1. And the π - π stacking part is also vital to the biological activity, showing more importance of the steric effect than electronic effect. In summary, we elaborated a series of FGFR inhibitors containing the novel scaffold of pyrrolo[2,3-b]pyrazine. This scaffold together with the interesting shape of this chemotype could benefit others to further develop selective FGFR inhibitors for cancer treatment.

Acknowledgments: We are grateful for financial support from the National Natural Science Foundation of China (Grant No. 81473243); NSFC-Shandong Joint Fund for Marine Science Research Centers (Grant No. U1406402); Youth Innovation Promotion Association and the “Personalized Medicines—Molecular Signature-based Drug Discovery and Development”, Strategic Priority Research Program of the Chinese Academy of Sciences, Grant No. XDA12020317).

Author Contributions: Bing Xiong, Yuchi Ma and Jing Ai designed the research; Yan Zhang, Yuchi Ma, Zhen Zhang, Ruifeng Wang, Tongchao Liu and Chaoyun Wang conducted the research; Hongchun Liu, Jing Ai, Jingkang Shen, Dongmei Zhao and Bing Xiong analyzed the data; Bing Xiong, Yuchi Ma, Jing Ai wrote the paper.

Conflicts of Interest: The authors declare no conflict of interest.

References

1. Katoh, M. Therapeutics targeting fgf signaling network in human diseases. *Trends Pharmacol.Sci.* **2016**, *37*, 1081–1096.
2. Parish, A.; Schwaederle, M.; Daniels, G.; Piccioni, D.; Fanta, P.; Schwab, R.; Shimabukuro, K.; Parker, B.A.; Helsten, T.; Kurzrock, R. Fibroblast growth factor family aberrations in cancers: Clinical and molecular characteristics. *Cell Cycle (Georgetown, TX)* **2015**, *14*, 2121–2128.
3. Ornitz, D.M.; Itoh, N. Fibroblast growth factors. *Genome Biol.* **2001**, *2*, 3005.
4. Ornitz, D.M.; Itoh, N. The fibroblast growth factor signaling pathway. *Wiley Interdiscip. Rev. Dev.Biol.* **2015**, *4*, 215–266.
5. Katoh, M.; Nakagama, H. Fgf receptors: Cancer biology and therapeutics. *Med.Res.Rev.* **2014**, *34*, 280–300.
6. Itoh, N.; Ornitz, D.M. Fibroblast growth factors: From molecular evolution to roles in development, metabolism and disease. *J. Biochem.* **2011**, *149*, 121–130.
7. Chae, Y.K.; Ranganath, K.; Hammerman, P.S.; Vaklavas, C.; Mohindra, N.; Kalyan, A.; Matsangou, M.; Costa, R.; Carneiro, B.; Villaflor, V.M.; et al. Inhibition of the fibroblast growth factor receptor (fgfr) pathway: The current landscape and barriers to clinical application. *Oncotarget* **2016**, doi:10.18632/oncotarget.14109.
8. Liang, G.; Liu, Z.; Wu, J.; Cai, Y.; Li, X. Anticancer molecules targeting fibroblast growth factor receptors. *Trends Pharmacol. Sci.* **2012**, *33*, 531–541.
9. Carter, E.P.; Fearon, A.E.; Grose, R.P. Careless talk costs lives: Fibroblast growth factor receptor signalling and the consequences of pathway malfunction. *Trends Cell Biol.* **2015**, *25*, 221–233.
10. Turner, N.; Grose, R. Fibroblast growth factor signalling: From development to cancer. *Nat. Rev. Cancer* **2010**, *10*, 116–129.
11. Saka, H.; Kitagawa, C.; Kogure, Y.; Takahashi, Y.; Fujikawa, K.; Sagawa, T.; Iwasa, S.; Takahashi, N.; Fukao, T.; Tchinou, C.; et al. Safety, tolerability and pharmacokinetics of the fibroblast growth factor receptor inhibitor azd4547 in japanese patients with advanced solid tumours: A phase I study. *Investig. New Drugs* **2017**, doi:10.1007/s10637-016-0416-x.

12. Goke, F.; Franzen, A.; Hinz, T.K.; Marek, L.A.; Yoon, P.; Sharma, R.; Bode, M.; von Maessenhausen, A.; Lankat-Buttgereit, B.; Goke, A.; et al. Fgfr1 expression levels predict bgj398 sensitivity of fgfr1-dependent head and neck squamous cell cancers. *Clin. Cancer Res.* **2015**, *21*, 4356–4364.
13. Taberero, J.; Bahleda, R.; Dienstmann, R.; Infante, J.R.; Mita, A.; Italiano, A.; Calvo, E.; Moreno, V.; Adamo, B.; Gazzah, A.; et al. Phase I dose-escalation study of jnj-42756493, an oral pan-fibroblast growth factor receptor inhibitor, in patients with advanced solid tumors. *J. Clin. Oncol.* **2015**, *33*, 3401–3408.
14. Patani, H.; Bunney, T.D.; Thiyagarajan, N.; Norman, R.A.; Ogg, D.; Breed, J.; Ashford, P.; Potterton, A.; Edwards, M.; Williams, S.V.; et al. Landscape of activating cancer mutations in fgfr kinases and their differential responses to inhibitors in clinical use. *Oncotarget* **2016**, *7*, 24252–24268.
15. Ma, Y.; Sun, G.; Chen, D.; Peng, X.; Chen, Y.L.; Su, Y.; Ji, Y.; Liang, J.; Wang, X.; Chen, L.; et al. Design and optimization of a series of 1-sulfonylpyrazolo[4,3-b]pyridines as selective c-met inhibitors. *J. Med. Chem.* **2015**, *58*, 2513–2529.
16. Guagnano, V.; Furet, P.; Spanka, C.; Bordas, V.; le Douget, M.; Stamm, C.; Brueggen, J.; Jensen, M.R.; Schnell, C.; Schmid, H.; et al. Discovery of 3-(2,6-dichloro-3,5-dimethoxy-phenyl)-1-[6-[4-(4-ethyl-piperazin-1-yl)-phenylamino]-pyrimidin-4-yl]-1-methyl-urea (nvp-bgj398), a potent and selective inhibitor of the fibroblast growth factor receptor family of receptor tyrosine kinase. *J. Med. Chem.* **2011**, *54*, 7066–7083.
17. Cheng, W.; Wang, M.; Tian, X.; Zhang, X. An overview of the binding models of fgfr tyrosine kinases in complex with small molecule inhibitors. *Eur. J. Med. Chem.* **2017**, *126*, 476–490.
18. Yan, W.; Wang, X.; Dai, Y.; Zhao, B.; Yang, X.; Fan, J.; Gao, Y.; Meng, F.; Wang, Y.; Luo, C.; et al. Discovery of 3-(5'-substituted)-benzimidazole-5-(1-(3,5-dichloropyridin-4-yl)ethoxy)-1H-indazoles as potent fibroblast growth factor receptor inhibitors: Design, synthesis, and biological evaluation. *J. Med. Chem.* **2016**, *59*, 6690–6708.
19. Zhang, Z.; Zhao, D.; Dai, Y.; Cheng, M.; Geng, M.; Shen, J.; Ma, Y.; Ai, J.; Xiong, B. Design, synthesis and biological evaluation of 6-(2,6-dichloro-3,5-dimethoxyphenyl)-4-substituted-1H-indazoles as potent fibroblast growth factor receptor inhibitors. *Molecules (Basel, Switzerland)* **2016**, *21*, doi:10.3390/molecules21101407.
20. Saladino, G.; Gervasio, F.L. New insights in protein kinase conformational dynamics. *Curr. Top. Med. Chem.* **2012**, *12*, 1889–1895.
21. Wang, Z.; Cole, P.A. Catalytic mechanisms and regulation of protein kinases. *Methods Enzymol.* **2014**, *548*, 1–21.
22. Wang, Q.; Zorn, J.A.; Kuriyan, J. A structural atlas of kinases inhibited by clinically approved drugs. *Methods Enzymol.* **2014**, *548*, 23–67.

Sample Availability: Samples of the compounds are available from the authors.



© 2017 by the authors. Licensee Preprints, Basel, Switzerland. This article is an open access article distributed under the terms and conditions of the Creative Commons by Attribution (CC-BY) license (<http://creativecommons.org/licenses/by/4.0/>).